SLAC–PUB–4624
May 1988
T/E

PROBING THE GAUGE STRUCTURE OF Z' BOSON AT A HIGH ENERGY e^+e^- COLLIDER*

B. W. LYNN

Stanford Linear Accelerator Center
Stanford University, Stanford, California 94309

and

Department of Physics
Stanford University
Stanford, CA 94305

and

R. G. STUART

Max Planck Institute for High Energy Physics
and Astrophysics
Munich, West Germany

and

M. CVETIČ

Department of Physics
University of Pennsylvania
Philadelphia, PA 19104

Submitted to *Nuclear Physics B*

* Work supported by the Department of Energy, contract DE–AC03–76SF00515.
† Work supported by NSF, contract PHY-86-12280

ABSTRACT

We show that the polarization asymmetry, A_{LR} on top of a new Z' is independent of the Higgs structure for sufficiently large $M_{Z'}$. It is explained how this fact can be used in conjuction with measurements of polarized forward-backward asymmetries and total cross-sections to rule out candidate extended gauge structures or symmetry breaking scenarios.

Linear e^+e^- colliders with a center of mass energy up to 1 TeV are currently under consideration as part of the next generation of particle accelerators.[1] In this paper we show how such a machine could be used to investigate the structure of the electroweak gauge group. A scenario is proposed in which evidence of a second massive neutral gauge boson, Z' is obtained by a future hadron collider or by precision measurements at LEP or SLC,[2] but that only an approximate value for its mass is determined. An e^+e^- collider of sufficient energy can then be used to scan the region of interest. Indeed for e^+e^- collisions at 1 TeV, say, initial state bremsstrahlung is so severe in the presence of a Z' resonance below 1 TeV that the machine's effective energy gets shifted down to the pole. We show here that it is possible to unambiguously distinguish between candidates for the extended electroweak gauge group from measurements with polarized beams on the Z'. In particular the groups $SU(2)_R \times SU(2)_L \times U(1)$ and $SU(2)_L \times U(1) \times U(1)$ will be considered. Of course, consideration of the latter would require that no charged W' had been observed. In a recent paper, Lynn and Cvetič[2]gave expressions for the currents of these gauge groups among others. These depend on a large number of parameters most of which relate to the Higgs sector. It turns out that measurements can be made that are largely insensitive to the Higgs structure. A similar thing has been observed to happen already in the case of the standard model and we review this using the approach given by Lynn, Peskin and Stuart.[3] On the Z^0 resonance the matrix element for a 4-fermion process is given by,

$$\mathcal{M}(-M_Z^2) = e^2QQ' - 24\pi \frac{(I_3 - Qs_\theta^2)(I_3' - Q's_\theta^2)}{i\Sigma_f[(I_3 - Qs_\theta^2)_L^2 + (I_3 - Qs_\theta^2)_R^2]} . \qquad (1)$$

Here the unprimed quantities apply to incoming particles primes denote outgoing particles. I_3 is the 3-component of weak isospin, Q is the electric charge and $\sum_f$ extends over all fermion species which are assumed massless. The possibility of decay into W^+W^- pairs,[4] light Higgs and exotic particles has been ignored. Thus the total cross–section, normalized to QED muon pair production, is

$$\frac{\sigma(q^2 = -M_Z^2)}{\sigma(e^+e^- \to \gamma^* \to \mu^+\mu^-)} = \frac{\Sigma_f[|\mathcal{M}_{LL}|^2 + |\mathcal{M}_{RR}|^2 + |\mathcal{M}_{LR}|^2 = |\mathcal{M}_{RL}|^2]}{64\pi^2\alpha_{em}^2} . \qquad (2)$$

The matrix elements on the r.h.s. of (2) represent the four contributing helicity amplitudes. Dropping the photon exchange term gives,

$$\frac{\sigma(q^2=-M_Z^2)}{\sigma(e^+e^-\to\gamma^*\to\mu^+\mu^-)}=\frac{9}{\alpha_{em}^2}\,\frac{(I_3-Qs_\theta^2)_{e_L}^2+(I_3-Qs_\theta^2)_{e_R}^2}{\Sigma_f[(I_3-Qs_\theta^2)_{f_L}^2+(I_3-Qs_\theta^2)_{f_R}^2]}\,. \tag{3}$$

Here $s_\theta^2\equiv\sin^2\theta_W$. Now since the Z current is given by $J_Z=I_3-Qs_\theta^2$ equation (3) can be written,

$$\frac{\sigma(q^2=-M_Z^2)}{\sigma(e^+e^-\to\gamma^*\to\mu^+\mu^-)}=\frac{9}{\alpha_{em}^2}\,\frac{(J_Z^{e_L})^2+(J_Z^{e_R})^2}{\Sigma_f[(J_Z^{f_L})^2+(J_Z^{f_R})^2]}\,. \tag{4}$$

Thus on top of Z^0 resonance the result clearly depends only on the Z current to $O(M_Z^2/M_{Z'}^2)$.

Similarly for a new neutral gauge boson Z' with mass $M_{Z'}$ and $M_Z/M_{Z'}\ll 1$ the analagous result is,

$$\frac{\sigma(q^2=-M_{Z'}^2)}{\sigma(e^+e^-\to\gamma^*\to\mu^+\mu^-)}=\frac{9}{\alpha_{em}^2}\,\frac{(J_{Z'}^{e_L})^2+(J_{Z'}^{e_R})^2}{\Sigma_{m_f<M_{Z'}/2}[(J_{Z'}^{f_L})^2+(J_{Z'}^{f_R})^2]}\,. \tag{5}$$

Now consider the case where the extended gauge group is $SU(2)_R\times SU(2)_L\times U(1)$. The electric charge is assumed to be given by,

$$Q=I_{3L}+I_{3R}+\frac{B-L}{2} \tag{6}$$

and for the Higgs field ϕ_i the vacuum expectation value has the property $Q\langle\phi_i\rangle=0$. In the usual way the fermion kinetic terms in the extended Lagrangian yield gauge invariant currents,

$$\begin{aligned}\overline{\psi}\not{D}\psi=g_L J_{3L}W_{3L}&+\frac{g_{B-L}g_R}{\sqrt{g_R^2+g_{B-L}^2}}\,(J_{3R}+J_{(B-L)/2})B'\\&+\sqrt{g_R^2+g_{B-L}^2}\left[J_{3R}-\frac{g_{B-L}^2}{g_R^2+g_{B-L}^2}\,(J_{3R}+J_{(B-L)/2})\right]Z'\\&+\text{derivative terms}\,.\end{aligned} \tag{7}$$

The Z' eigenstate is identifiable since it has,

$$\langle I_{3L}^2 \rangle = 0 \qquad \langle I_{3L} I_{3R} \rangle = 0 \qquad \langle I_{3R}^2 \rangle \neq 0 \tag{8}$$

again under the assumption that $M_Z \ll M_{Z'}$. One obtains,

$$Z' = \frac{1}{\sqrt{g_R^2 + g_{B-L}^2}} \left(g_R W_{3R} + g_{B-L} B \right) \tag{9}$$

and two (approximately) massless orthogonal states,

$$W_{3L}, \qquad \frac{1}{\sqrt{g_R^2 + g_{B-L}^2}} \left(g_{B-L} W_{3R} + g_R B \right) . \tag{10}$$

Hence the Z' current

$$J_{Z'} \propto J_{3R} - \frac{\xi}{1-\xi} J_{(B-L)/2} \tag{11}$$

where,

$$\xi = \frac{g_{B-L}^2}{g_R^2 + g_{B-L}^2} .$$

To resolve this further one extracts the electric charge, Q, and weak mixing angle, θ_W by identifying the standard model Z^0 and photon. Notice that the hypercharge current is,

$$J_Y = J_{3R} + J_{(B-L)/2} \tag{12}$$

so that B' is the hypercharge field and $g' = g_{B-L} g_R / \sqrt{g_R^2 + g_{B-L}^2}$ is the hypercharge coupling. It follows from equations (11) and this last relation that,

$$\xi = \frac{g_L^2}{g_R^2} \tan^2 \theta_W . \tag{13}$$

Summarizing then,

$$J_{Z'} = J_{3R} - \frac{\xi}{1-\xi} J_{(B-L)/2} + 0\left(\frac{M_Z^2}{M_{Z'}^2}\right) \tag{14}$$

For e^+e^- collisions on the Z' peak we obtain from (14)

$$A_{LR}(-M_{Z'}^2) = \frac{-2(2\eta+1)}{1+(2\eta+1)^2} + 0\left(\frac{M_Z^2}{M_{Z'}^2}\right) . \tag{15}$$

where $\eta = \xi/(\xi-1)$.

Figure 1 shows $A_{LR}(-M_{Z^0}^2)$ an Z^0 resonance for two different Higgs structures *including all terms* $O(M_Z^2/M_{Z'}^2)$. For the reasons just discussed, when $M_Z/M_{Z'} \geq 5$ the dependence on the Higgs structure is small. Similarly $A_{LR}(-M_{Z'}^2)$ on Z' resonance will be fairly independent of Z^0 couplings for $M_{Z'}/M_{Z^0} > 5$.

A detailed study of the effective gauge structure will inevitably require the measurement of quantities that, unlike A_{LR}, depend on the quantum numbers of the final state particles, for example, the total cross-section, σ_{tot}, or the polarized forward-backward asymmetry, $A_{polFB}^{f\bar{f}}$. In order to limit the dependence of such quantities on the quantum numbers of, as yet, undiscovered fermions, we will restrict ourselves to final states involving the first three generations. In particular, with suitable microvertex detection, top and bottom quark events should be readily identifiable. Exotics can be eliminated through their higher mass by selecting topologies of high sphericity.[5] Only light neutrals coupling only to the Z' cannot be excluded in this way, but such particles do not naturally arise in most models. They will not be considered further. In all curves the weak angle $\sin^2\theta_W$ is taken to be 0.215. The ratio g_R/g_L is allowed to vary in the range 0.72—1.0. Figure 2a shows the total cross-section for production of $b\bar{b}$ on the Z' resonance in units of $\sigma(e^+e^- \to \gamma^* \to \mu^+\mu^-)$ plotted against the polarization asymmetry. Figure 2b shows the polarized forward-backward asymmetry for bottom quarks, $A_{polFB}^{b\bar{b}}$. i.e.

$$A_{polFB}^{b\bar{b}} = \frac{\sigma_L^F - \sigma_L^B - \sigma_R^F + \sigma_R^B}{\sigma_L^F - \sigma_L^B - \sigma_R^F + \sigma_R^B} \tag{16}$$

where $\sigma^{F(B)}_{L(R)}$ denotes the cross-section for production of the b quark into the forward (backward) hemisphere in $e^+e^-_{L(R)} \to b\bar{b}$. At tree level this quantity is independent of the initial state fermions. Figure 2c shows the production cross section for $t\bar{t}$ in the same units as for Fig. 2a. Figure 2d displays $A^{t\bar{t}}_{polFB}$. In Figure 2e the total production cross section for the first three generations is shown.

If the observed relation between the measured quantities does not fall on the plotted curves, then $SU(2)_R \times SU(2)_L \times U(1)$ is ruled out. If the measured value does lie in the curve, then this group is still ruled out if inconsistent values for the ratio are obtained from different curves. For a given symmetry breaking scenario the ratio g_R^2/g_L^2 is predicted by the renormalization group equations so that if the experimental data does lie consistently on the predicted curves, the quantity g_R^2/g_L^2 can be obtained unambiguously and a particular symmetry breaking scenario ruled in or ruled out.

Consider now the case of the gauge group $SU(2)_L \times U(1) \times U(1)$. Again, for sufficiently large $M_{Z'}/M_Z$ the couplings become independent of the Higgs' structure. This is illustrated in Fig. 3 where $A_{LR}(-M^2_{Z^0})$ is plotted to two different Higgs' structures in $SU(2)_L \times U(1) \times U(1)$. Here the situation is rather more complicated The two U_1's couple to fermions via terms of the form $g''Y''B'' + g'''Y'''B'''$ (with Y'' and Y''' hypercharges for the two $U(1)$ groups). These may mix to produce the usual hypercharge Y and hypercharge field, B, and an additional U_1 field, B', via a mixing angle we denote θ_{U_1}. That is to say,

$$g''Y''B'' + g'''Y'''B''' \to gYB + g'Y'B' \tag{17}$$

and

$$\begin{pmatrix} \cos\theta_{U_1} & \sin\theta_{U_1} \\ -\sin\theta_{U_1} & \cos\theta_{U_1} \end{pmatrix} \begin{pmatrix} Y'' \\ Y''' \end{pmatrix} = \begin{pmatrix} Y \\ Y' \end{pmatrix} . \tag{18}$$

If we plot the same set of curves as before for the case $SU(2)_R \times U(1) \times U(1)$ in Figures 4 a—d, a 2-parameter family of curves depending on $g_{Y''}/g_{Y'''}$ and θ_{U_1} is

obtained. The ratio $g_{Y''}/g_{Y'''}$ is allowed to vary in the range -2.8—3.0 and curves are plotted for $\theta_{U_1} = 0°$, 22.5°, 45°, 67.5°, 90°. Plotting against the polarization asymmetry tends to spread the curves, thereby increasing the sensitivity to the parameters and facilitating their extraction from experimental data. For clarity no attempt has been made to mark the values of $g_{Y''}/g_{Y'''}$ along the curves but it is easy to do so. We do not exclude the possibility that there are other pairs of quantities better suited for the extraction of $g_{Y''}/g_{Y'''}$ and θ_{U_1}. Any pair of curves can then be used to extract the values of these quantities. The third curve then0rules out gauge group $SU(2)_L \times U(1) \times U(1)$ if the prediction is inconsistent with the experimental measurement. Again for a given symmetry breaking scenario the ratio $g^2_{Y''}/g^2_{Y'''}$ is predicted through renormalization group equations and this may be used to exclude a particular scenario in the case when consistent values for both parameters are obtained. Note in particular that the curves in Figure 4d lie in a region inaccessible to $SU(2)_L \times SU(2)_R \times U(1)$ (cf. Figure 2d) and thereby provide an unambiguous means of distinguishing between the two groups.

CONCLUSIONS

We have shown that measurements of the polarization asymmetry, A_{LR}, provide a means of ruling out candidate extended gauge structures or symmetry breaking scenarios. Polarization of the electron beam is a useful tool here because since it not only give additional quantities that can be used to test predictions, but also improves the resolution of the parameters of the extended gauge structure. This, along with the polarization asymmetry's relative freedom from experimental uncertainties that plague most other quantities, make polarization a useful tool on top of a new Z'.

FIGURE CAPTIONS

1) The longitudinal polarization asymmetry, A_{LR}, on top of the Z^0 resonance as a function of $M_{Z'}/M_Z$ for two different Higgs structures for $SU(2)_L \times SU(2)_R \times U(1)_{B-L}$.

2) Various experimentally measurable quantities plotted against the polarization asymmetry on the Z' resonance for the gauge group $SU(2)_L \times SU(2)_R \times U(1)$. The ratio g_R/g_L varies from 0.72 to 1.0. $\sin^2\theta_W$ is taken to be 0.215 throughout.

   a) The production cross section for $b\bar{b}$ in units of $\sigma(e^+e^- \to \gamma^* \to \mu^+\mu^-)$

   b) The polarized forward–backward asymmetry, $A^{b\bar{b}}_{polFB}$, for $b\bar{b}$.

   c) The production cross section for $t\bar{t}$.

   d) The polarized forward–backward asymmetry, $A^{t\bar{t}}_{polFB}$, for $t\bar{t}$.

   e) The total production cross section for the first three fermion generations.

3) The longitudinal polarization asymmetry, A_{LR}, on top of Z^0 resonance as a function of

4) The same quantities as in Figures 2a—e but for the gauge group $SU(2)_L \times U(1) \times U(1)$. g''/g''' ranges from -2.8 to 3.0. $\theta_{U_1} = 0°$, (solid line); $\theta_{U_1} = 22.5°$, (dotted line); $\theta_{U_1} = 45°$, (dashed line); $\theta_{U_1} = 67.5°$, (dash/dot line); $\theta_{U_1} = 90°$, (solid line).

REFERENCES

1. C. Ahn, *et al.*, SLAC Report 329, May 1988
2. B. W. Lynn and M. Cvetič, SLAC-PUB-3900, 1986, Phys. Rev. D 35 (1987), p. 51
3. B. W. Lynn, M. E. Peskin and R. G. Stuart, In "Physics at LEP", CERN 86-02, eds. J. Ellis and R. Peccei.
4. C. Dib and F. Gilman, Phys. Rev. D 36 (1987), p. 1337
5. G. Feldman, Private communication.

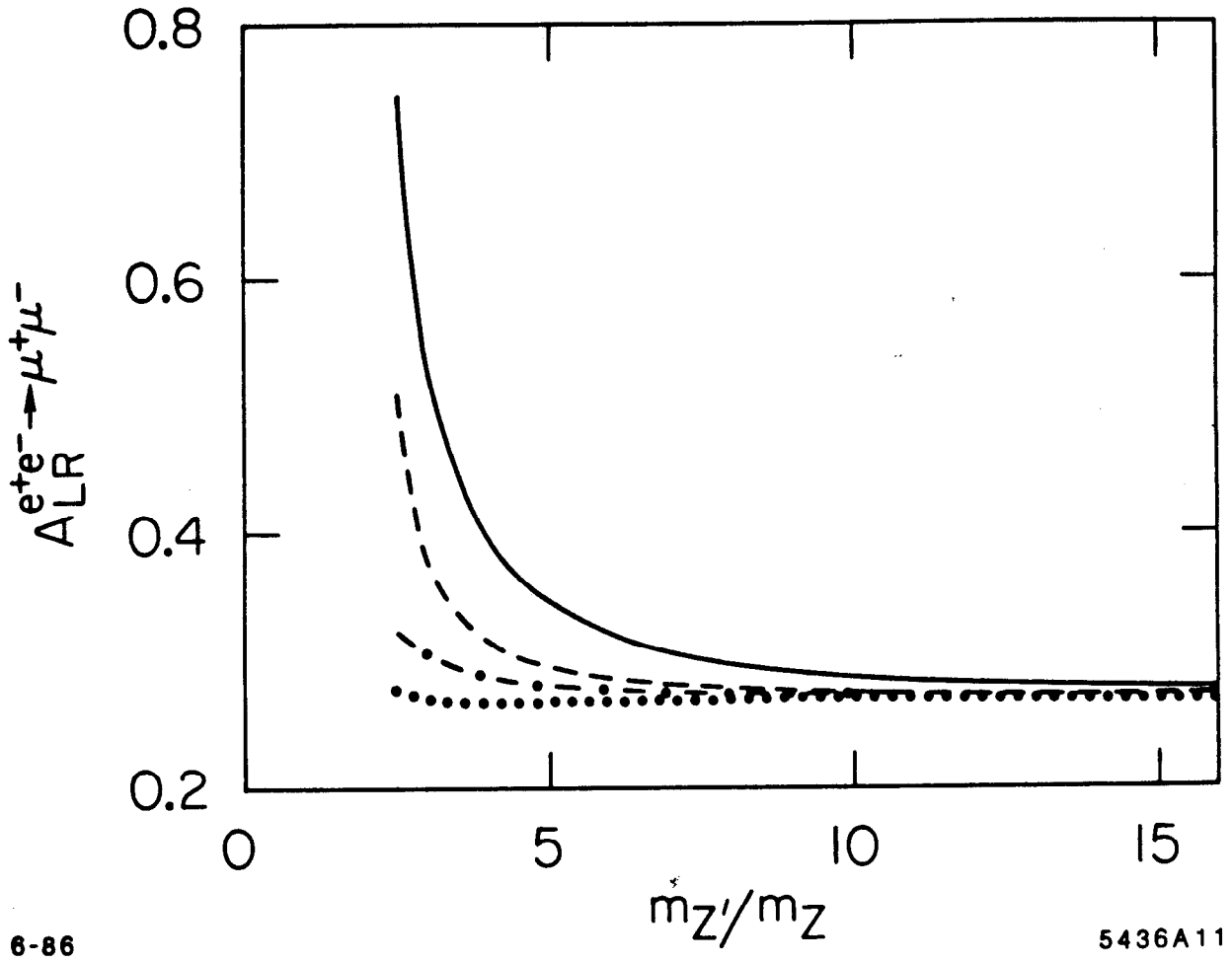

Fig. 1

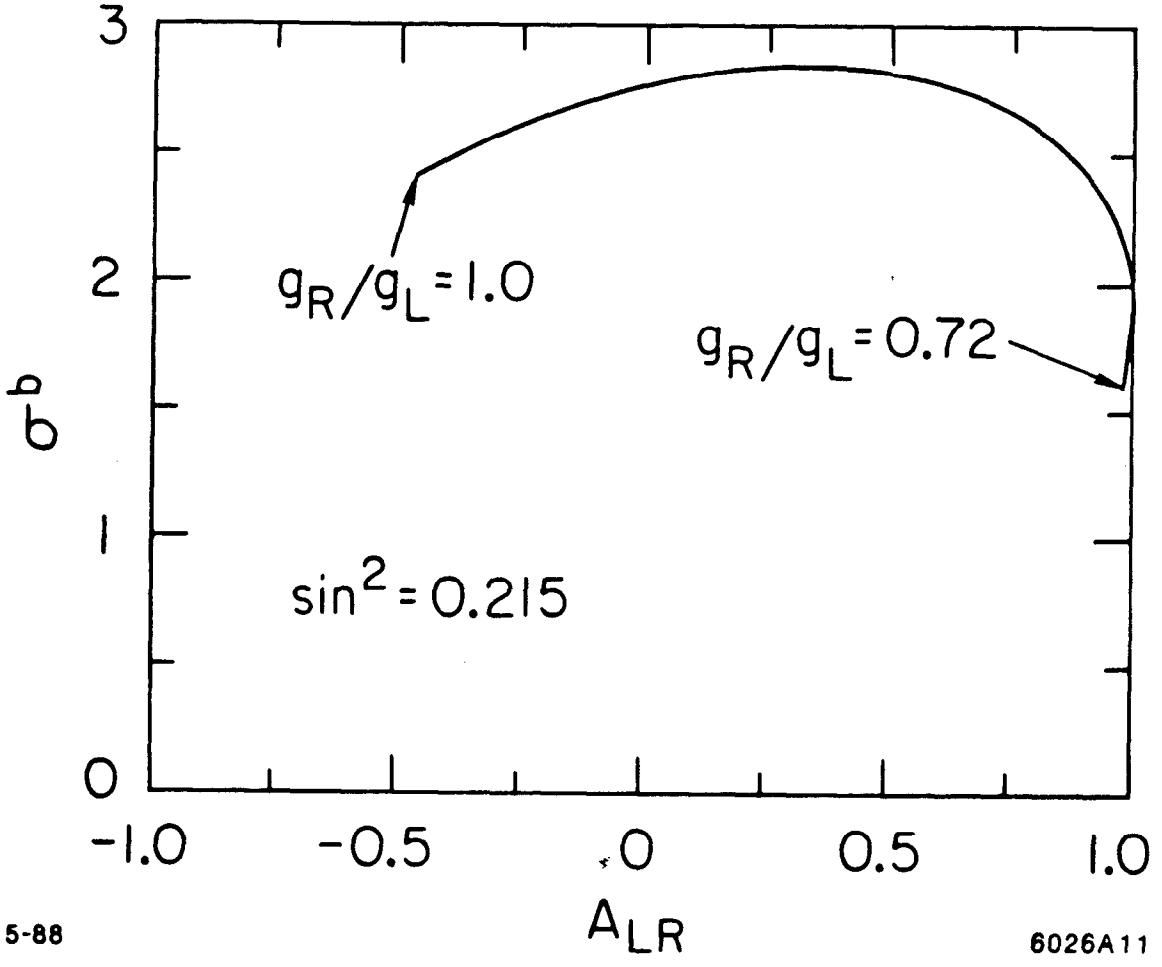

Fig. 2a

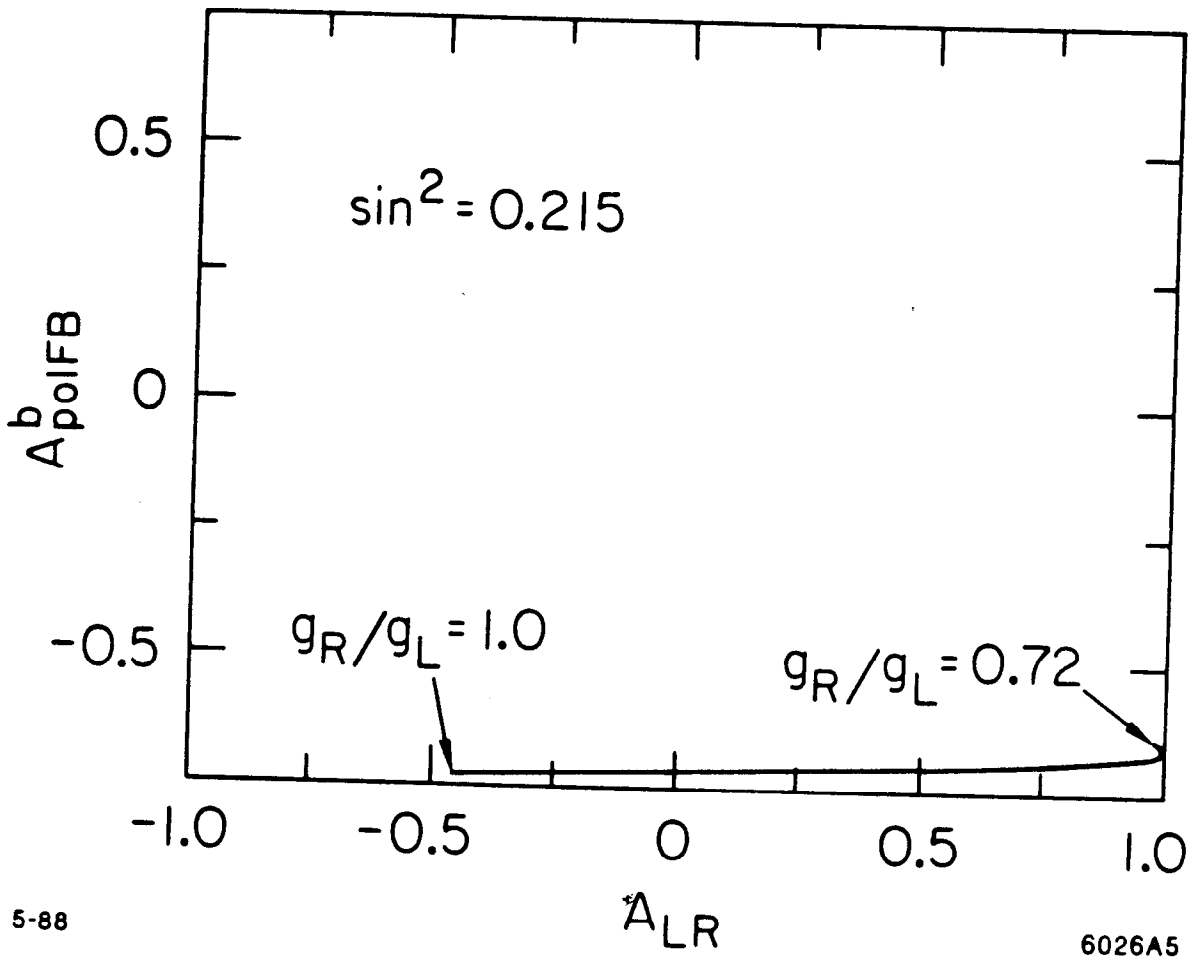
0.5
0
-0.5
A^b_{polFB}
$\sin^2 = 0.215$
$g_R/g_L = 1.0$
$g_R/g_L = 0.72$
-1.0
-0.5
0
0.5
1.0
A_{LR}
5-88
6026A5

Fig. 2b

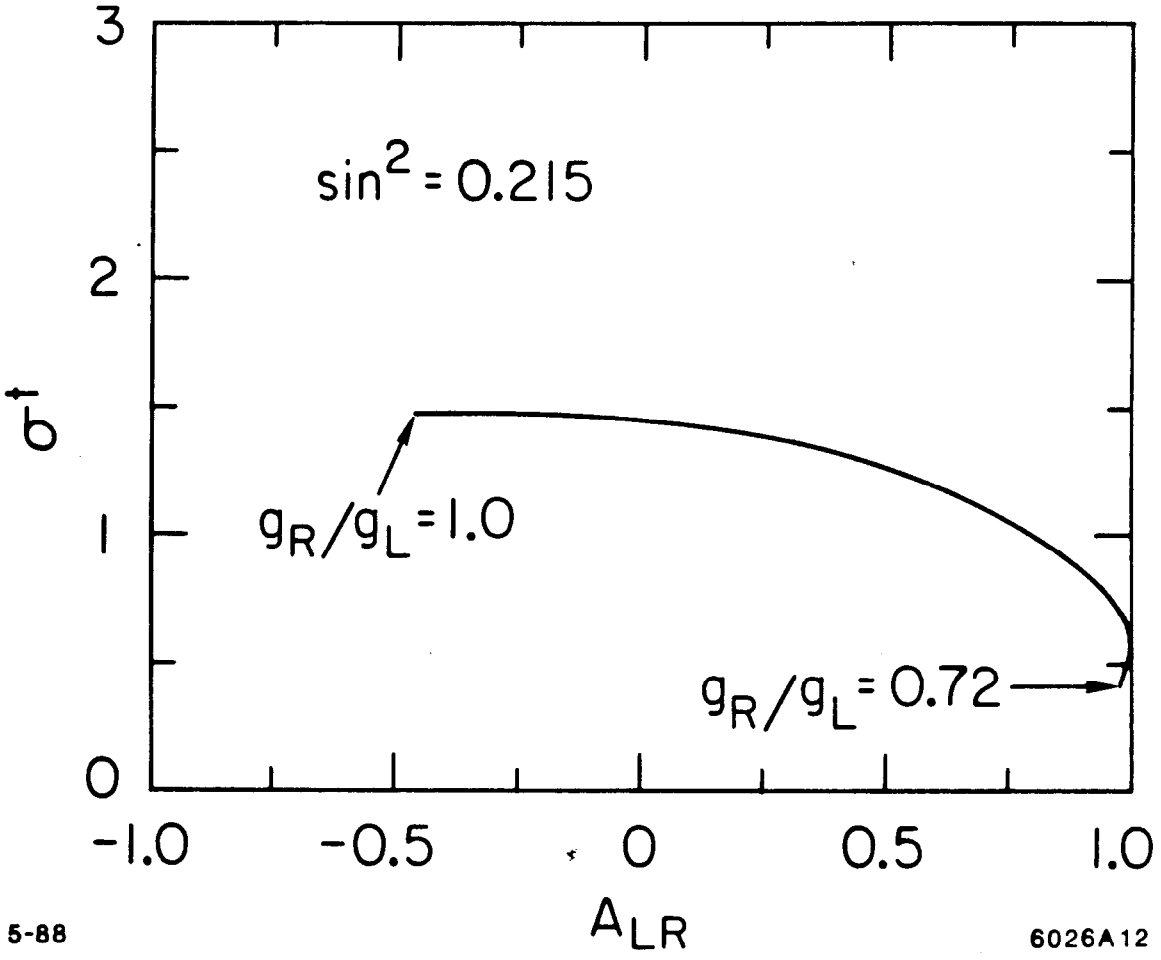
3
2
1
0
$\sin^2 = 0.215$
$\bar{b}$
$g_R/g_L = 1.0$
$g_R/g_L = 0.72$
-1.0
-0.5
0
0.5
1.0
A_{LR}
5-88
6026A12

Fig. 2c

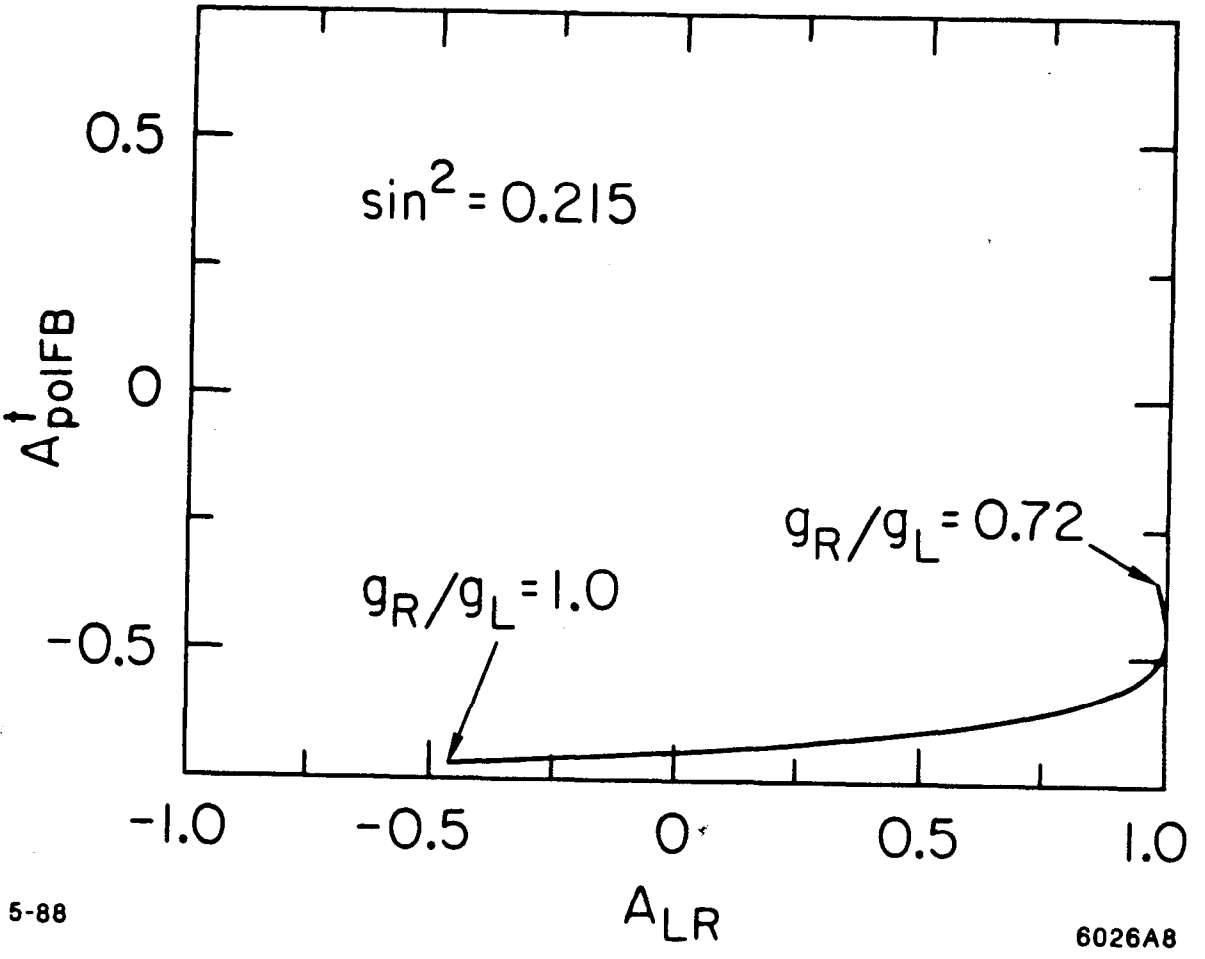
0.5
0
-0.5
A^t_{polFB}
$\sin^2 = 0.215$
$g_R/g_L = 0.72$
$g_R/g_L = 1.0$
-1.0
-0.5
0
0.5
1.0
A_{LR}
5-88
6026A8

Fig. 2d

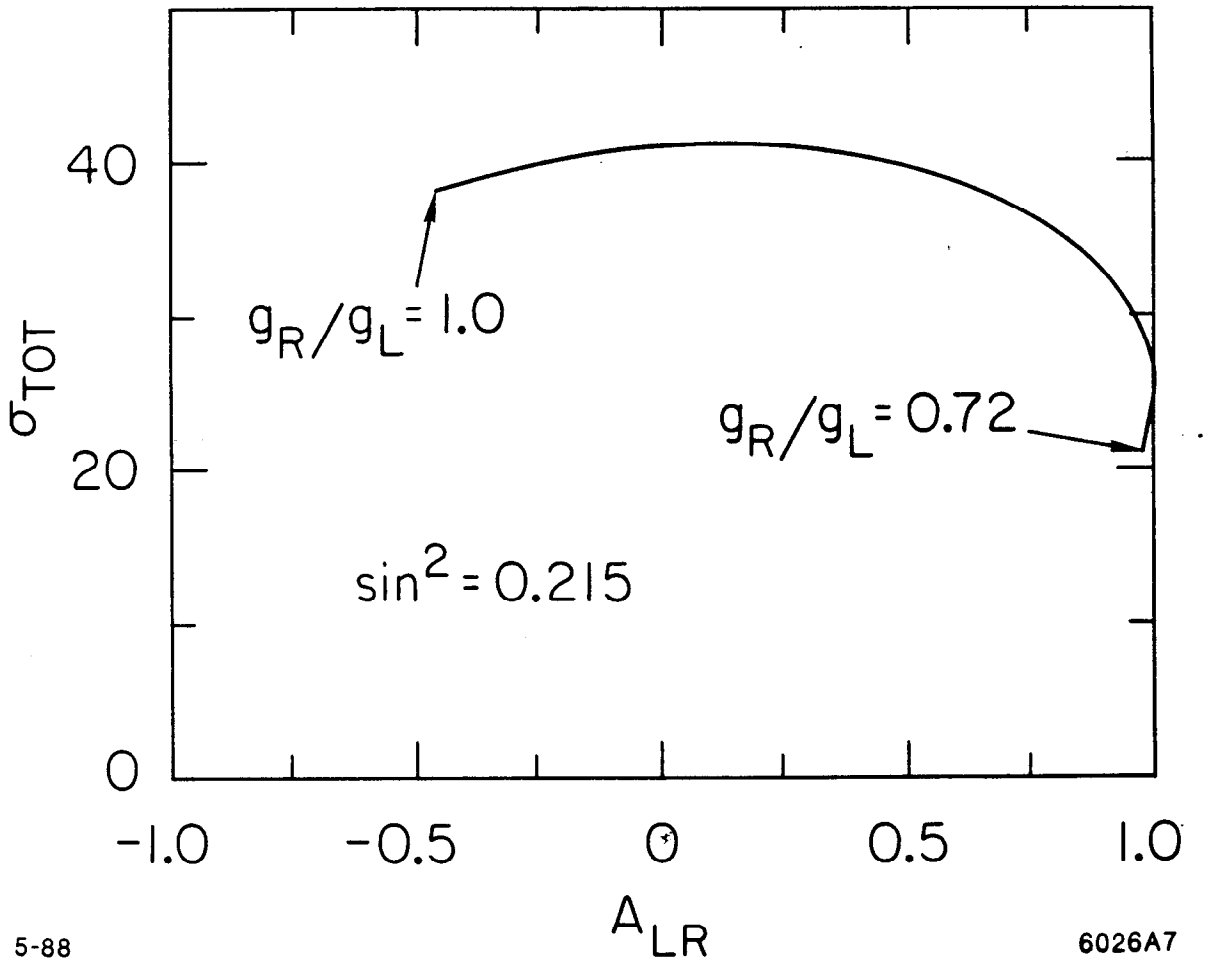
40
20
0
σ_{TOT}
$g_R/g_L = 1.0$
$g_R/g_L = 0.72$
$\sin^2 = 0.215$
-1.0
-0.5
0
0.5
1.0
A_{LR}
5-88
6026A7

Fig. 2e

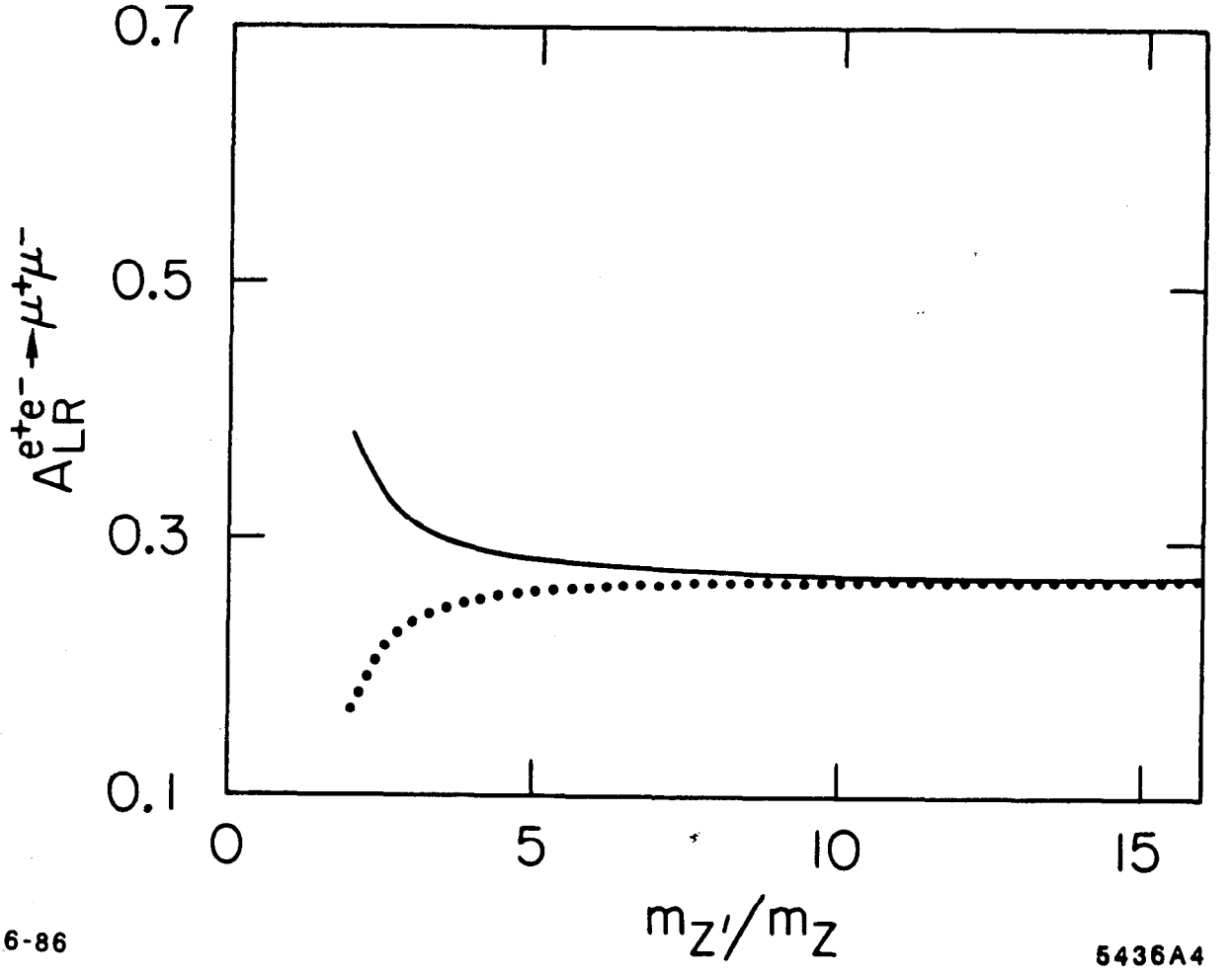

Fig. 3

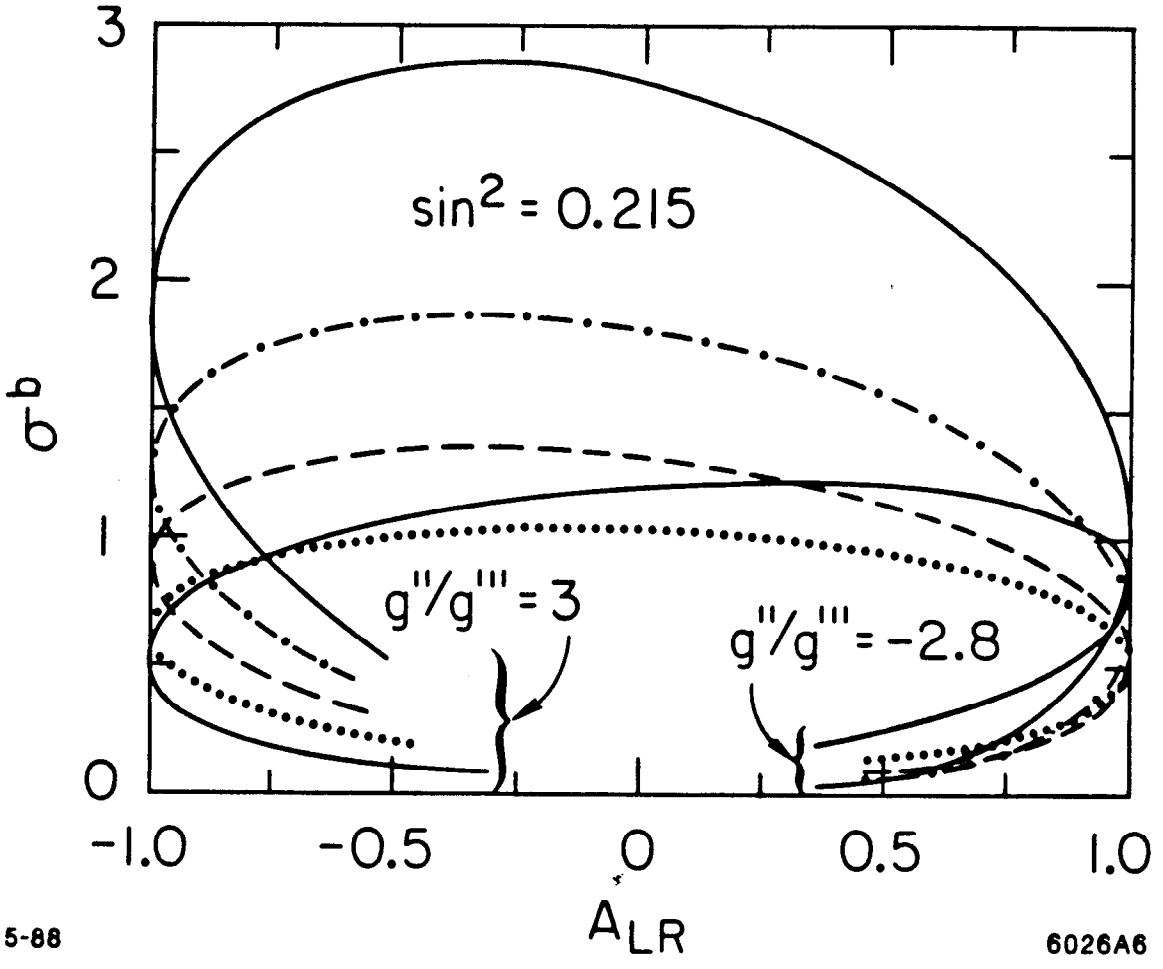

Fig. 4a

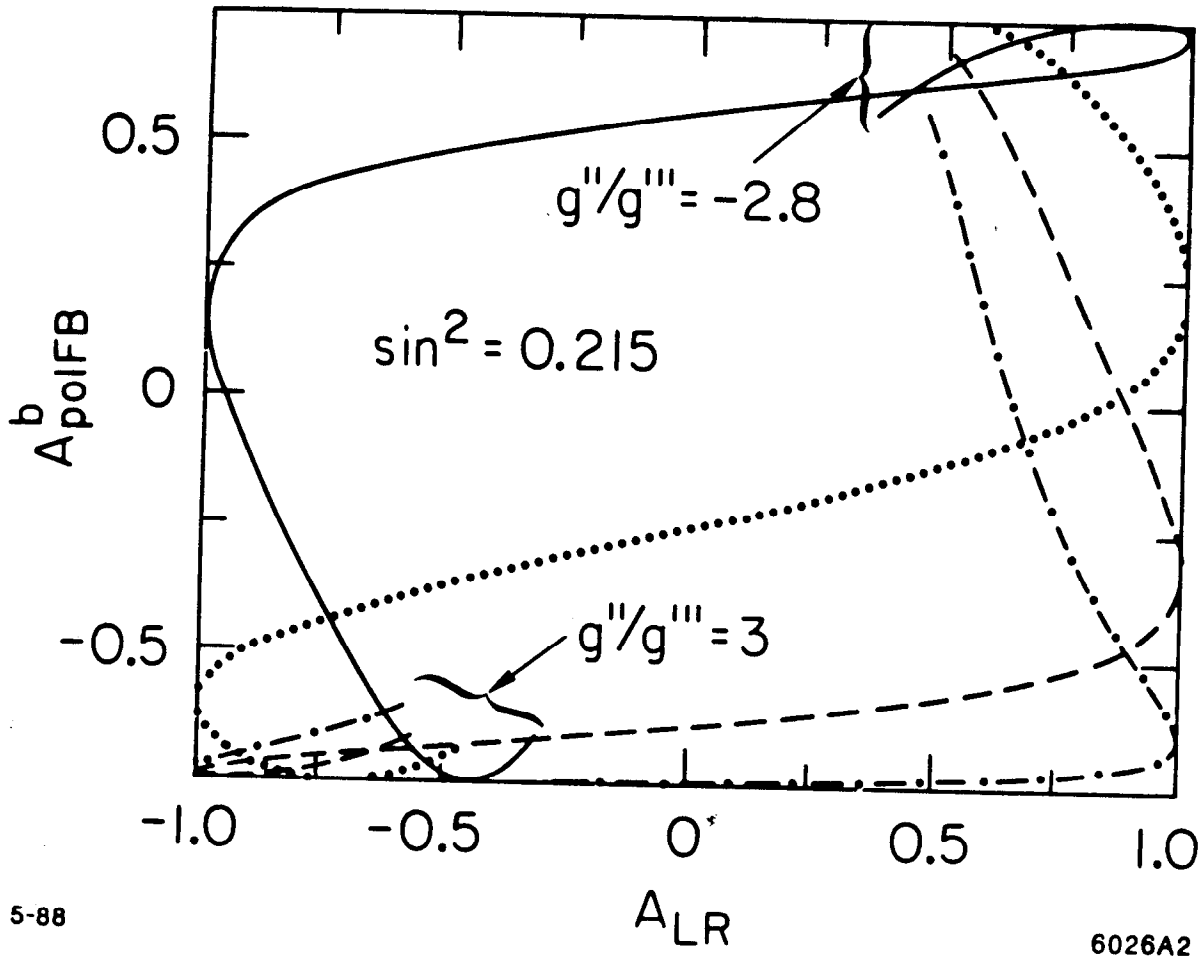

Fig. 4b

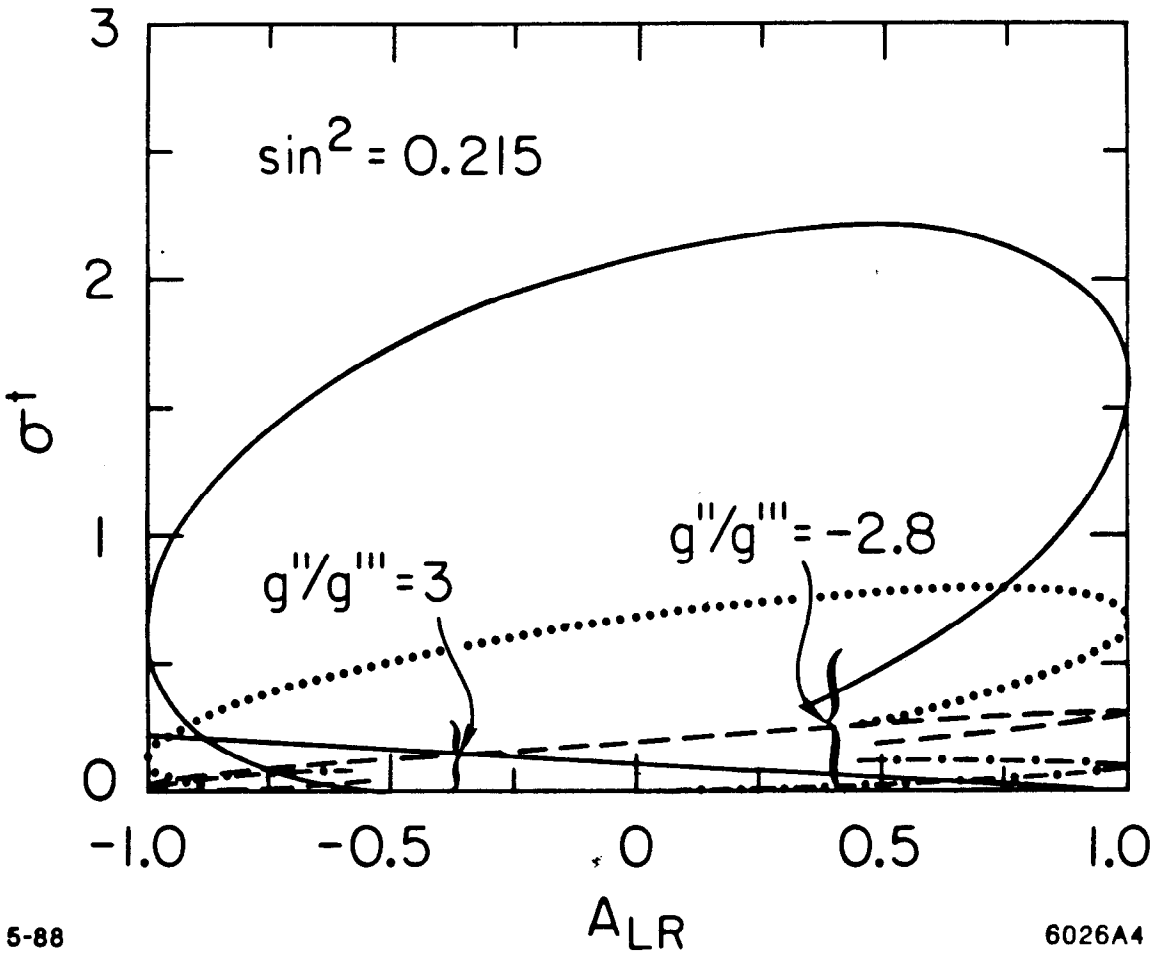

Fig. 4c

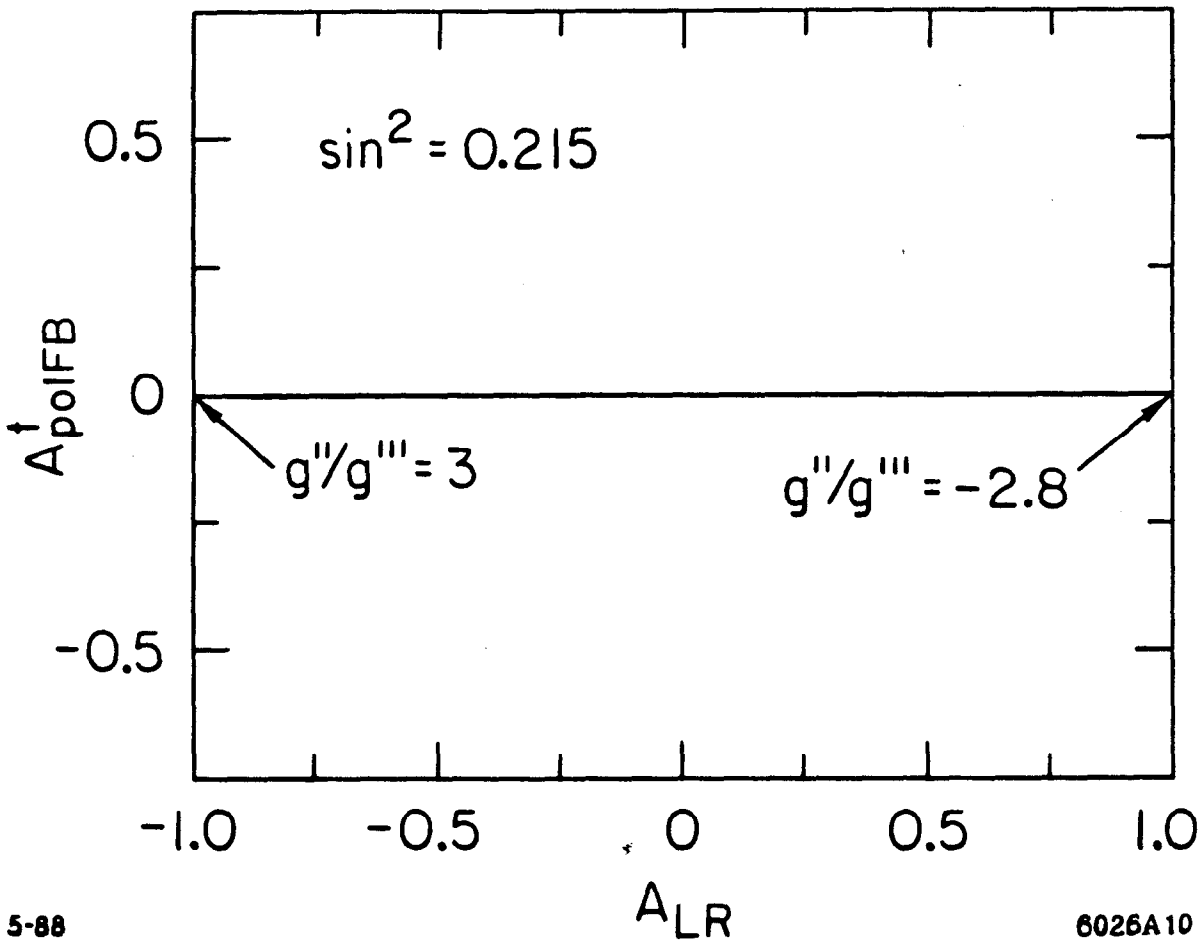

Fig. 4d

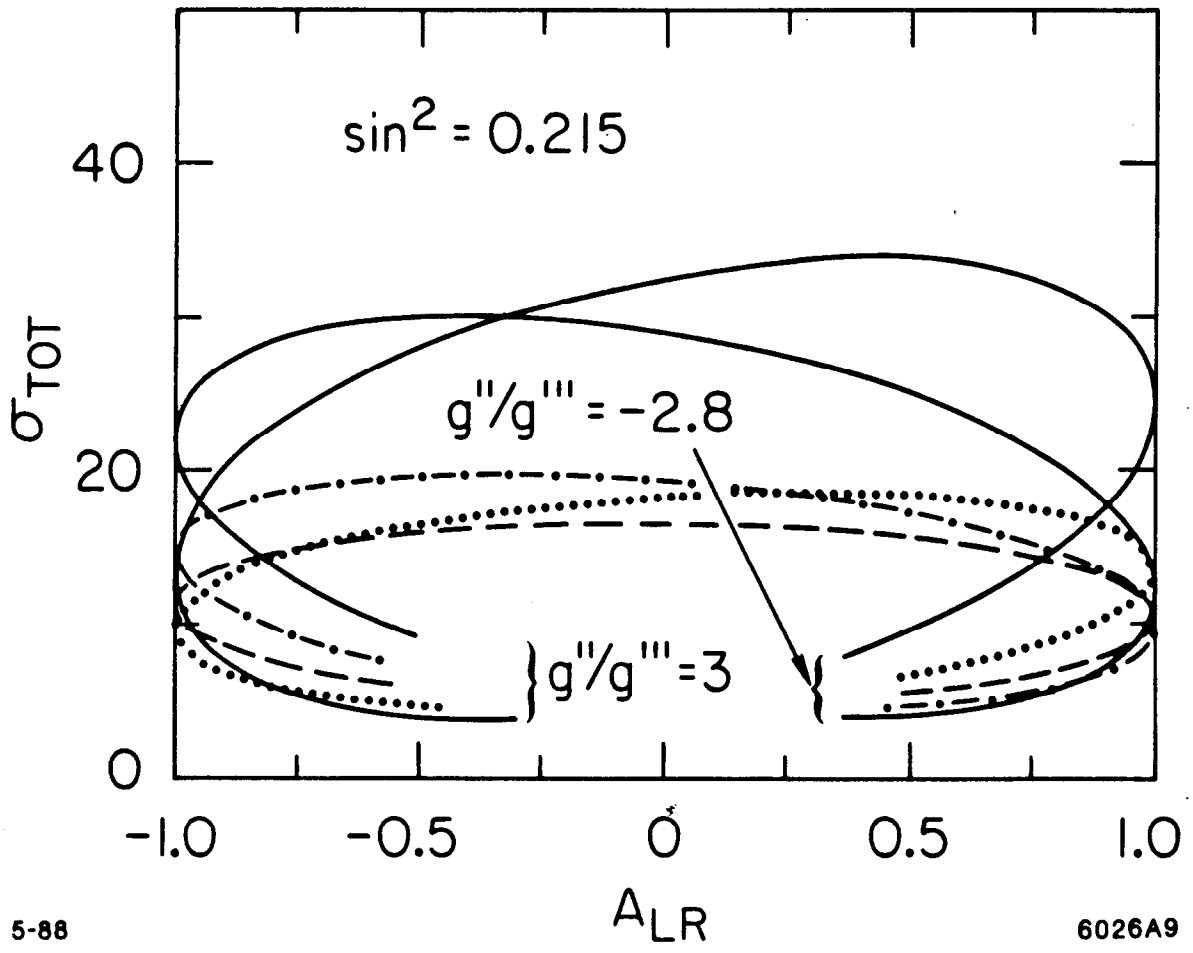

Fig. 4e